Antifertility Effect of Iron A- Fe2O3 with Poly Aniline and Gamma- Ray (Γ-Ray) on Epididymis Sperm for Mice

Bydaa T. Sih

University of Baghdad , College of Science , Department of Physics , Baghdad, Iraq, beedo_taher@yahoo.com

In the present study, within the realm of physical and chemical experimentation, polyaniline was synthesized at two different concentrations (0.02 and 0.04 grams) under ambient conditions using the chemical polymerization technique. The attributes of the resultant compound were examined via FTIR, XRD, and SEM analyses, uncovering a distinct peak in the FTIR spectrum ranging from 1470 to 1560. This synthesized compound exhibits various potential applications, particularly in the field of medical research, and in investigating the impacts of Fe2O3 at concentrations of 0.04 and 0.02 grams. The biological segment of the investigation involved the preparation and categorization of thirty mice into eight distinct groups. The outcomes of the study, conducted over a period of 5 weeks, demonstrated a notable reduction in testosterone levels along with decreased sperm motility and count. Notably, animals subjected to α-Fe2O3 exhibited a significant increase in abnormal sperm count ($P < 0.05$) independent of any magnetic field influence. Moreover, there was a noteworthy enhancement ($P < 0.05$) in sperm motility and concentration, live sperm percentage, and testosterone levels. Conversely, a substantial decline ($P < 0.05$) was observed in the proportion of abnormal sperm within the PANI-treated group. The combination of PANI-α-Fe2O3 revealed sensitivity to a magnetic field compared to the α-Fe2O3 group devoid of any magnetic field. Mice treated solely with PANI displayed enhancements across all measured parameters, except for the percentage of abnormal sperm which exhibited a significant reduction ($P < 0.05$).

Keywords: Conductive polymer, Fe2O3/PANI, nanoparticle composite, cancel activities, Gamma-ray, sperm.

1. Introduction

Since its initiation in the 1990s, nanotechnology has undergone rapid expansion in various industrial and technical domains, along with its notable practical implementations. Forecasts indicate that the nanotechnology sector could reach a market value of $3.7 trillion by 2015 (Research and Markets, Dublin 2008). Owing to the favorable perspective, academia,

governmental bodies, and private enterprises exhibit a strong interest in conducting research activities and promoting commercial applications within the realm of nanoscale science and technology. A crucial element of this effort entails nurturing an environment conducive to increased patent submissions, which serves as the foundation of the nanotechnology discipline. The core principle behind innovative progress in nanoscale materials and technology frequently pertains to the synthesis of artificial powders. Certain companies and research establishments contend that the specific complexities of manufacturing processes and associated equipment embody valuable proprietary information, leading to a disparity between the current volume of patents issued in the nano powder sector and the practical industrial feasibility of these substances. Patent endeavors originating from diverse nations focus on the production of materials at the nanometer scale. While a significant portion of patents related to nanoscale powders originates from entities situated in the United States, Japan, and Europe, there is a noticeable upsurge in patent applications emerging from China, Australia, India, and Korea. Chemical synthesis stands as the primary technique employed for generating nanoscale powders (refer, for example, to US 7572430 B2, US 6054495 B2, US 5747180 B2, and CN 00129483).

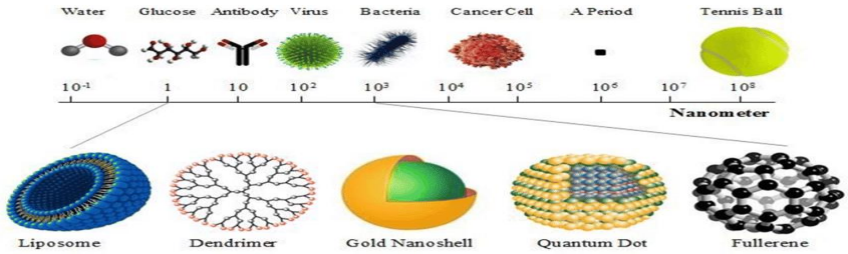

Figure 1 Nanoscale and nanostructures.

Nanotechnology has exhibited considerable potential within the sphere of healthcare and medical science. At present, a plethora of severe and intricate illnesses pose a significant risk to human well-being, encompassing conditions like diabetes, cancer, Parkinson's disease, Alzheimer's disease, cardiovascular diseases, multiple sclerosis, as well as various serious inflammatory or infectious diseases such as HIV. Nanomedicine, as a subdivision of nanotechnology, is actively employed in the realms of medical and health sectors, utilizing nanomaterials and nano electrical biosensors. The progress in molecular nanotechnology is positioned to receive backing from the advancements in nanomedicine, offering hopeful prospects for the global population. The utilization of nanoscience in medical intervention carries immense promise for all human populations, delivering numerous advantages. Nanomedicine facilitates early detection and prevention of diseases, enhanced diagnosis, personalized therapy, and effective post-treatment procedures. In addressing ailments such as cancer, bacterial infections, and inflammation, hyperthermia, also referred to as thermotherapy, subjects biological tissues to heightened temperatures to eradicate diseased cells or pathogens by disrupting proteins and cell membranes. Conventional hyperthermia techniques entail exposure to heat or the utilization of heated blankets, in addition to the administration of heated saline solution through catheters. A variety of heating techniques like microwave and ultrasonic strategies are in existence, despite frequently demonstrating invasiveness and having the potential to cause harm to healthy tissues. Non-invasive

approaches like inductively coupled magnetic fields, radiofrequencies, and near-infrared (NIR) light have been examined to surmount the constraints of traditional hyperthermia. The production of the composite -Fe_2O_3/PANI-cysteine through an innovative technique devised in this investigation tackles the unavoidable toxicity linked with medicinal substances. This study delves into the impact of magnetic fields and Fe_2O_3 concentration in polyaniline on the treatment of cancer cells at a microscopic scale.

2. Experimental I work

Table(1) shows the reagents and materials used in this study

Table(1) explain the Reagents and materials

NO.	Chemical Materials	Purity	Supplier
1	Sperm of mice	99%	Laboratory synthesis
2	Ammonium Persulphate $(NH_4)_2S_2O_8$	98%	Himedia-India
3	L-cysteine I ($C_6H_{12}N_2O_4S_2$)	98%	Bimedia-India
	Iron III (αFe_2O_3)	98%	Himedia-I India
8	Dimethyl I Sulfoxide (DMSO) $(CH_3)_2SO$	99.6%	BDH-England I

The different areas that investigate potential uses of nanotechnology comprise: a. Healthcare and Medical Science b. Electronics c. Transportation d. Energy and Environmental Science e. Aerospace exploration

Delivery Of Drugs

Nanoparticles play an essential role within the realm of nanotechnology, particularly in the context of precise drug delivery. Through the specific targeting of affected areas, this methodology ensures the precise administration of required dosages while minimizing potential adverse reactions. The employment of this highly discriminating approach holds promise in reducing costs and alleviating patient discomfort. As a result, a variety of nanoparticles including dendrimers and nanoporous materials are currently in use. Micelles derived from block co-polymers are employed for the encapsulation of pharmaceuticals, facilitating the conveyance of small drug molecules to their designated sites. Moreover, nano electromechanical systems are utilized for the regulated release of medications. Notably, the applications of iron nanoparticles and gold shells in cancer treatment are of considerable significance. The adoption of targeted drug delivery leads to diminished drug intake and healthcare expenses, ultimately enhancing the. quality of patient care

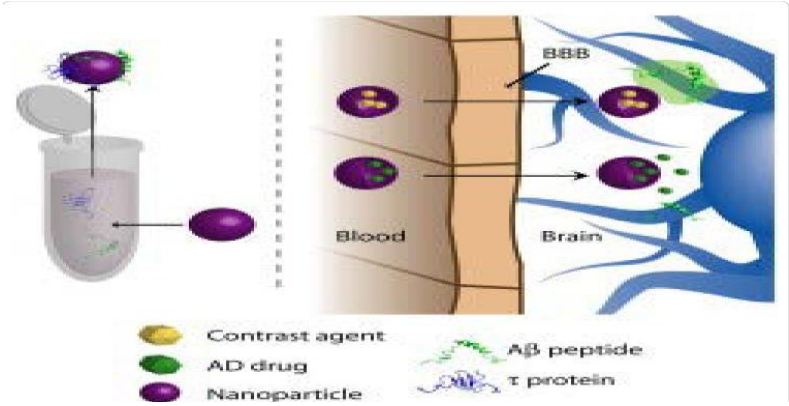

Figure 2 showed the Use of nano particles in human disease.

Nanoparticles play a pivotal role in the oncology field, especially in imaging, due to their small size. The utilization of magnetic resonance imaging allows nanoparticles such as quantum dots to produce high-quality images of tumors, thanks to their size-dependent light emission properties. Quantum dots, brighter than organic dyes, require only one light source for activation, making them a cost-effective choice as contrast agents. Despite their benefits, it is crucial to acknowledge that quantum dots often contain toxic elements. The synthesis process of Iron oxide Fe_2O_3 Hypered Ani electronic I scale began with measuring 0.45ml of aniline using an I scale, then diluting it with 50ml of deionized water to achieve a one I mole concentration. Fe_2O_3 (0.02 and 0.05 g) was then added in a two-to-one iron I ratio to the mixture in a flask, which was stirred continuously and placed in an ice bath at 3C for 15 minutes I. Simultaneously, a solution of 4.5 grams of ammonium peroxy disulphate (APS) with a concentration of 1M was prepared by diluting it in 50 ml of distilled water I, maintaining stable conditions through stirring and cool temperatures. The APS solution was slowly added to the aniline solution, causing the clear granular mixture to turn into a dark I green-tinted solution. After purification through vacuum I the following I day, the mixture was washed with distilled water, filtered, and dried in an oven at 80°C for four hours. Once the powder was confirmed dry, mortars were used to grind it into a fine powder for I further diagnostic I analyses

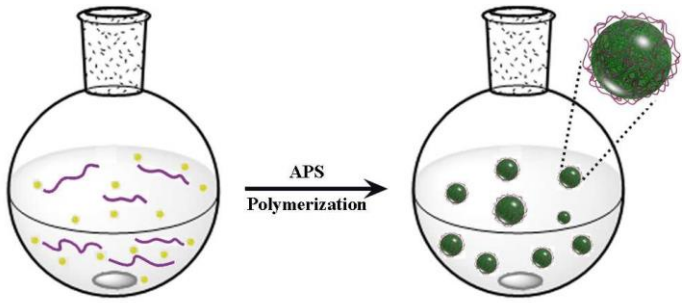

.

Figure 3 show the Fe_2O_3- NPs are created in accordance with Scheme 1 (counterions have been eliminated for clarity).

3. Experimental Animals:

In the present investigation, 32 white Swiss mice, aged between 10 to 8 weeks, and with an average weight ranging from 30 to 25 g, were utilized. These mice were subjected to an infection with the MTX cancer type. Housing arrangements involved placing the mice in plastic cages with sawdust-covered floors. Subsequently, the animals were segregated into eight distinct groups, with each group comprising 4 animals as specified in the biological examinations table. Upon completion of the designated research duration, the animals underwent euthanasia through cervical dislocation. Post euthanasia, the animals were dissected via an abdominal cavity incision in an inverted T configuration. The excision of the epididymis ensued, accompanied by the removal of adherent fatty tissues. The excised tissue was then dried using filter paper and submerged in a physiological saline solution for subsequent analyses. The assessments involved the determination of a-motility and sperm density. For the evaluation of sperm motility and density, a specific volume of the cauda epididymis was procured using 0.2 ml of physiological saline. Following a five-minute interval post-sacrifice, a drop of the homogenized sample was positioned on a glass slide, covered with a glass coverslip. The quantification of spermatozoa per designated area was conducted to ascertain the percentage of motile spermatozoa. Utilizing conventional methodologies, the cauda epididymal sperm count was computed and reported in million/mm3 of suspension.

N. sperms /ml= $\frac{n*400*200}{80*0.1}$ ……. (1)

$$\frac{\text{Dead/live or abnormal sperm count}}{\text{total sperm count}} * 100\%$$

b- The measurement of testosterone concentration: Blood sample collection: Utilizing a 1 ml syringe, blood samples were obtained from the animal through the method of heart stabbing, known for its immediacy and directness in sample acquisition, prior to euthanasia.Centrifugation process: Subsequent to blood procurement, the samples underwent centrifugation at a speed of 2000 revolutions per minute (rpm) for a duration of 10 minutes. This centrifugal step aids in the segregation of blood constituents, particularly serum, from other components like red blood cells. Storage of serum: Post serum isolation, it was preserved at a temperature of -20°C. This crucial measure is essential for maintaining sample integrity and inhibiting hormone deterioration until quantification. Quantification of hormone levels: The assessment of hormone concentrations within the serum will involve the utilization of specialized analytical instruments such as the Mini Vidas, designed specifically for measuring diverse hormones in biological specimens, alongside a suite of instruments tailored for this specific task.

Gamma –ray source

A gamma cell -900 irradiation device is used for the irradiation experiments. This device is manufactured by (Bahbha Atomic Research Center in Bombay, India /Well-Type device). It is used as a source of gamma rays (γ-rays). The radioactive source is Cobalt-60 (^{60}Co). The device is designed as a cylindrical container in which the samples are placed, with the rods protruding from the radioactive source. The control of the inputs and outputs of the container

is electricity facilitated, with the dosage controlled by a stopwatch included in the device. To ensure safety, the device is surrounded by a protective lead shield and is located in a room constructed of bricks and cement in the Department of Physics at the Faculty of Science at Baghdad College. The radiation dose rate emitted by the radioactive source inside the cylinder was measured with a scrub at 850Gy/h. This scrub is used to measure the radiation dose to radioactive sources by measuring the concentration of ferric ions produced from ferrous iron when it is exposed to ionizing radiation. The specific solution used for this purpose consists of dissolving 0.1g of ferrous ammonium sulfate in a mixture of 0.8 normal sulphuric acid and 25ml of sodium chloride (NaCl 10^{-2}mol), which is then diluted to a volume of 250ml with ion-free distilled water.

4. Result and discussion

The chemical composition of the hybrid nanocomposites of PANI and PANI-Fe2O3 (0.02 and 0.05 g) was validated by Fourier transform infrared spectroscopy (FTIR). PANI FTIR spectrum of PANI (Fig. 1) shows the carbon skeleton peak at 1121 cm-1 and the C-N stretching peak at 1292 cm-1, along with the C-H out of the aromatic ring at position 1.4 position in the intrinsic PANI out-of-plane. The pronounced peak at 1470 cm-1 is a consequence of the C=C stretching of the benzenoid ring, while the peak at 1559 cm-1 signifies the high doping level of the PANI. N-H stretching vibrations at 3428 cm-1 can also be observed. The well-defined peaks identified provide substantial evidence for the synthesis of PANI.

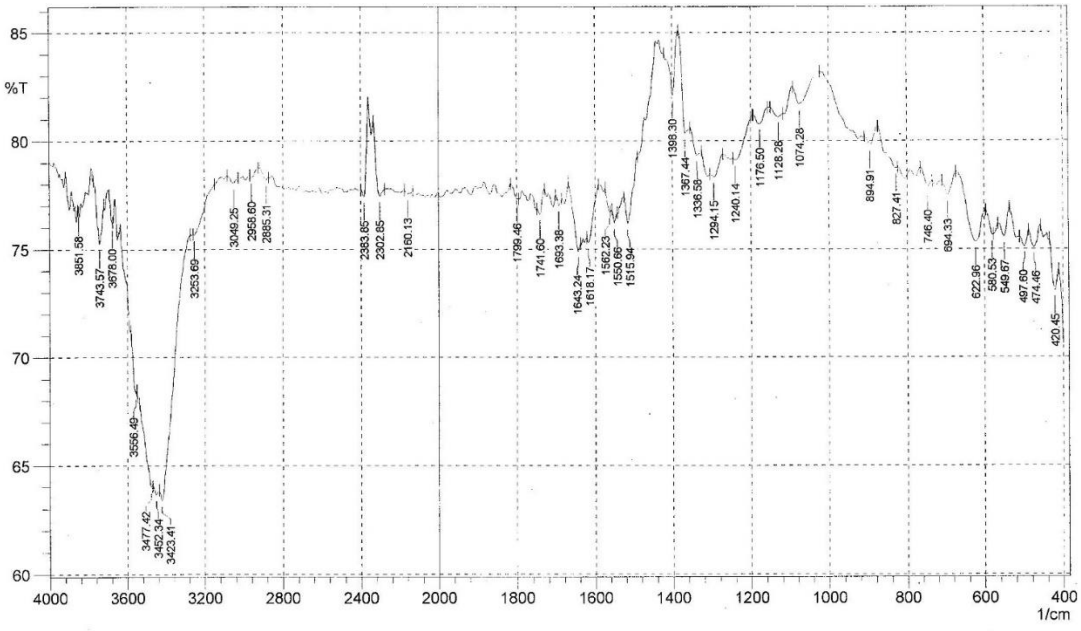

Figure (1): FTIRIII spectraIII of PANIIIII.

The chemical composition of the hybrid nanocomposites of PANI and PANI-Fe2O3 (0.02 and 0.05 g) was validated by Fourier transform infrared spectroscopy (FTIR). PANI FTIR spectrum of PANI (Fig. 1) shows the carbon skeleton peak at 1121 cm^{-1} and the C-N stretching peak at 1292 cm^{-1}, along with the C-H out of the aromatic ring at position 1.4 position in the intrinsic PANI out-of-plane. The pronounced peak at 1470 cm^{-1} is a consequence of the C=C stretching of the benzenoid ring, while the peak at 1559 cm^{-1} signifies the high doping level of the PANI. N-H stretching vibrations at 3428 cm-1 can also be observed. The well-defined peaks identified provide.

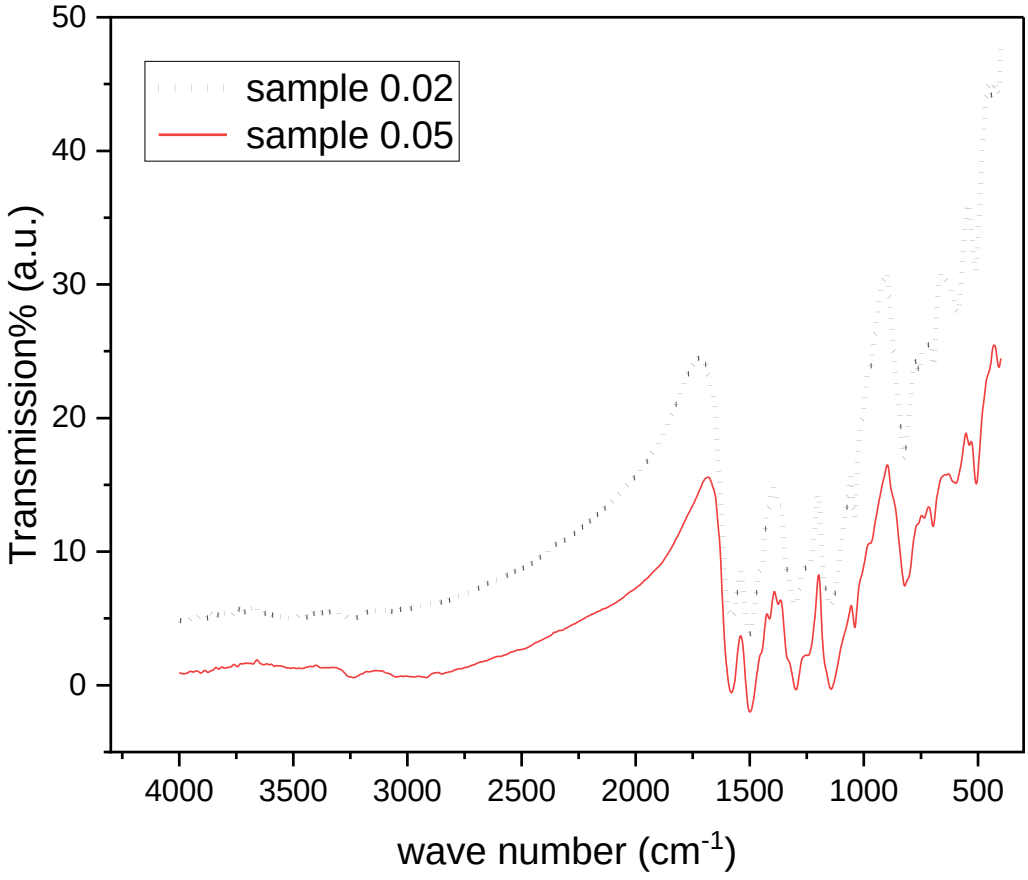

Figure (2) The Fe_2O_3PANI-Cys FTIR spectral areas.

The SEM images offer valuable insights into the morphology and structure of the hybrid nanocomposites formed by Fe_2O_3 and PANI. An explanation rooted in scientific principles sheds light on the following observations: Polymerization Selectivity: Aniline exhibits selective polymerization on Fe_2O_3 particles, with the degree of polymerization being influenced by the ratio of Fe_2O_3 to aniline. A higher ratio results in reduced PANI coverage on the spherical Fe2O3 particles, while a lower ratio leads to thicker PANI coatings and the attachment of PANI particles to Fe_2O_3 Color Variation: The intensity of color in the composites is directly related to the concentration of Fe_2O_3. A higher Fe_2O_3concentration

imparts a deeper brown hue to the composite, reflecting the amount of PANI bonded to the Fe_2O_3 particles. Microporosity and Interfacial Area: A very microporous structure is indicated by the strong bonding seen in all samples between the PANI layer and the Fe2O3 particles. Because it increases the space between the liquid and solid phases, this microporosity is beneficial and may improve the material's performance in applications such as sensing or catalysis. FE-SEM Examination: Field emission-scanning electron microscopy (FE-SEM) is used to analyze the properties of the material in more detail. Femtosecond-scanning electron microscopy (FE-SEM) confirms the exceptional characteristics of Fe2O3-PANI hybrid nanocomposites by generating pictures with better resolution and offering a more thorough evaluation of surface features. Understanding the nanoscale interaction between Fe2O3 and PANI and how it affects the overall characteristics of the composite material is made possible in large part by these results. The capacity to control the Fe2O3:aniline ratio.

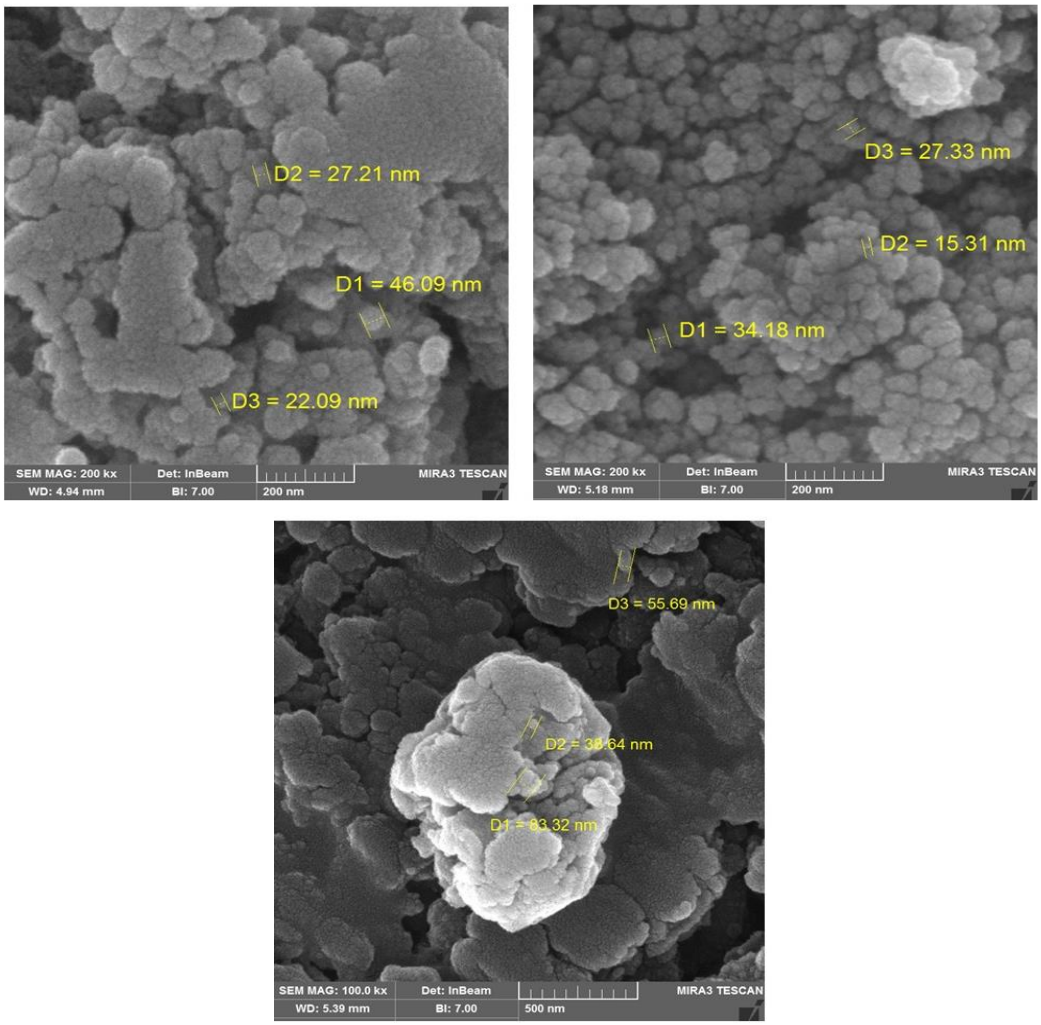

Figure 3. SEM for Fe_2O_3PANI-Cys

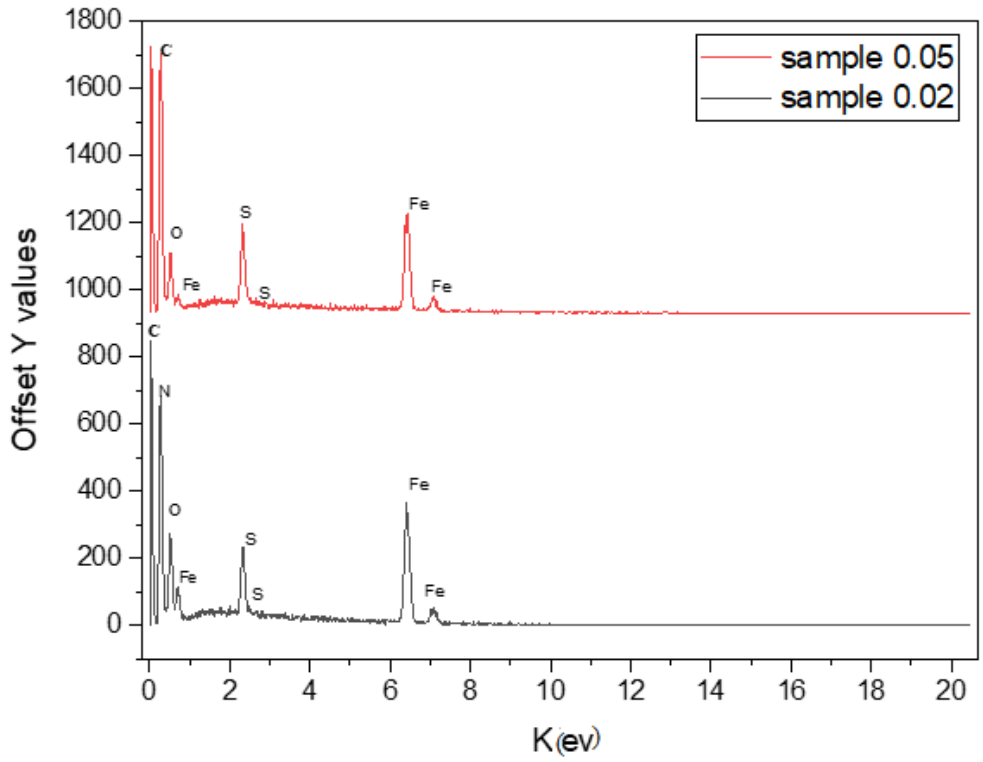

Figure 4.EDX analysis for Fe_2O_3 PANI-Cysteine

Table1 . the proportions for chemical elements

Elt	Line	Int	K	Kr	W%	A%	ZAF
C	Ka	178.4	0.439	0.189	44.19	58.39	0.42
N	Ka	13.8	0.046	0.019	13.53	15.33	0.14
O	Ka	77.2	0.094	0.040	19.54	19.38	0.20
S	Ka	73.7	0.0425	0.018	2.14	1.06	0.85
Fe	Ka	177.4	0.377	0.163	20.6	5.85	0.79

The result of sperm test

The motility and liveness percentages of sperm in Table (1) demonstrate a significant reduction ($P<0.05$) in sperm motility, liveness, and concentration percentages for the group treated by PANI-Fe_2O_3 compared to the control group. Furthermore, there was a notable increase ($P<0.05$) close to the control group in the group treated with pure PAN and exposed to PANI-Fe_2O_3 (0.05) compared to the PANI-Fe_2O_3 exposed group (0.02). Additionally, the group that underwent PANI treatment showed an enhancement in the proportion of sperm motility.

Abnormal Sperm Ratio

When compared to the control I group, the mice exposed to I PANI-Fe_2O_3 had a significantly higher percentage of sperm that were malformed (P<0.05). The proportion of sperm that were distorted was significantly lower (P<0.05) in the group of mice treated with PANI pure and exposed to PANI-Fe_2O_3 (0.05gm) compared to the group of mice exposed to PANI-Fe2O3 (0.02gm). The final PANI-treated group performed somewhat similarly to the control group in terms of the percentage of sperm with aberrant shapes.

Table (1) show the sperm motility, dead and abnormalities sperm under exposure effect γ-Ray

Parameter I s Groups I	Motility I % (mean±SD) I	Dead I % (mean±SD)	Abnormalities I % (mean±SD) I	I Count $\times 10^7$ I (mean±SD)
Neg.control	A 88.98±3.591	F 14.132±1.488	F 15±3	A 33.033±2.906
MTX	D 56.34±2.62	A 39±1.65	A 27.33±2.52	E 16±2
MTX±	C 64.933±4.51	B 27.833±1.98	AB 24±3.1	E 16±2
MTX±Irone 0.02	C 68.831±2.906	B C24±3	BC 23.327±2.01	E 18.06±1.202
MTX±Iron 0.05	C 69±1.92	CD 22±2	CD 20.333±1.528	CD 23.333±1.528
MTX±Polymar (0.02)± γ-Ray	B 78.967±4.51	DE 21.01±1.95	D 20±3.02	D 21.86±1.97
MTX±Polymar (0.05)± γ-Ray	A 87.06±3.08	DE 20±2	DE 18.123±1.528	BC 24.999±1.498
MTX±Polymarpure± γ-Ray	A 89±3.061	E 18±2	EF 15±2	BC 27.67±3.06
LSD	7.021	4.171	3.385	4.112
P-value	«0.0005	«0.0005	«0.00005	«0.00005

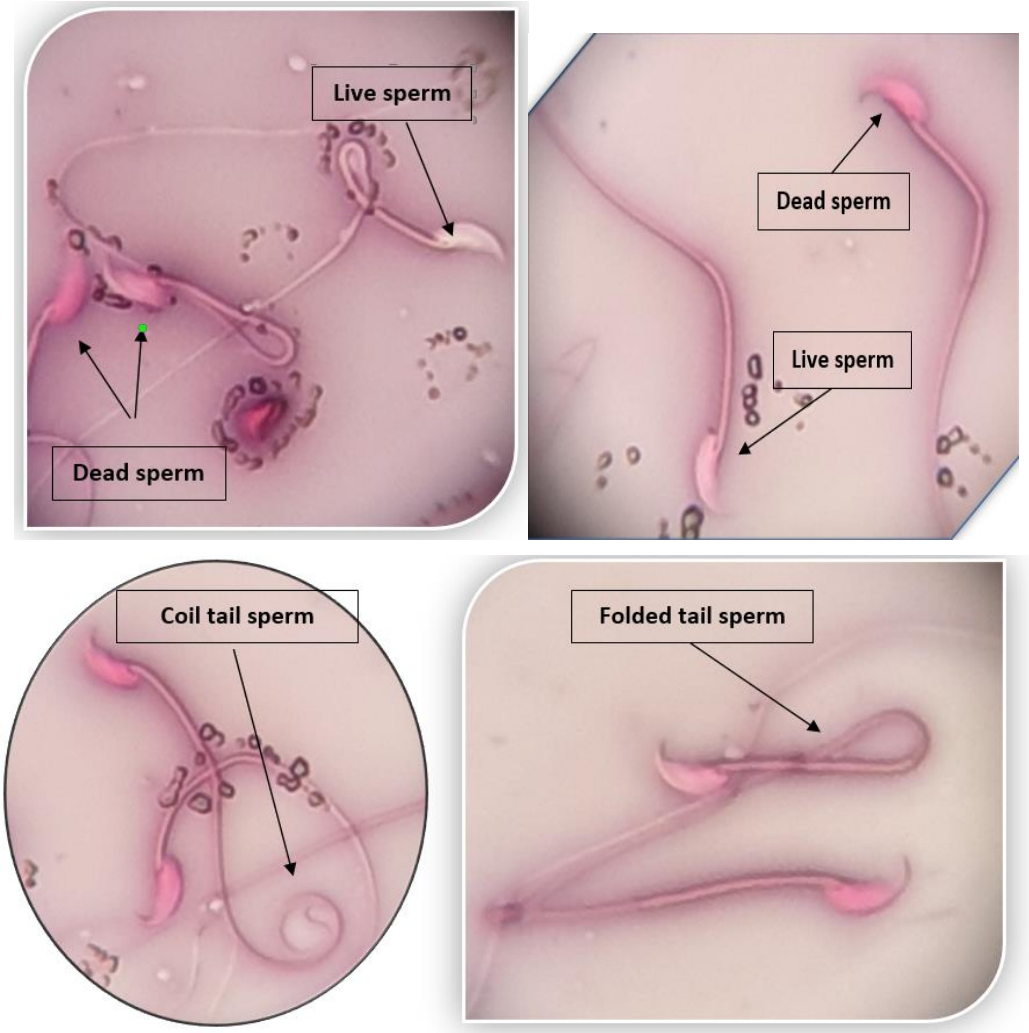

Figure (3) show the sperm a-Dead sperm which take eosin stain and abnormal tail (Coil & folded tail sperm). Slide stained with Nigrosin and Eosin stain (100x) b- Dead sperm which take eosin stain and live normal sperm no take eosin stain. With normal tail. Slide stained with Nigrosin and Eosin stain (100x)

Concentration of Testosterone

The concentration of testosterone was analyzed, showing (Table 2) a significant decrease in levels within the group exposed to PANI-Fe2O3 compared to those not exposed (control group). The mean level of testosterone increased notably after this change in the PANI pure-treated mice group exposed to Fe_2O_3 (0.05) when contrasted with the Fe_2O_3-exposed mice group (0.02), and it was also increased in the PANI and PANI- Fe_2O_3 treated mice group (0.05) compared to the control group.

Table (2) show the sperm Testosterone hormone under exposure effect γ-Ray

Parameters / Groups	Testosterone ng/ml (mean±SD)	FSH mIU/ml (mean±SD)	LH mIu/ml (mean±SD)
Neg.control	A 4.9552±0.09333	E 2. 978±0.2098	D 2.707±0.346
MTX	F 4.0043±0.206	A 6.002±0.4001	A 3.962±0.297
MTX+Lasser	E 4.0873±0.1077	B 5.126± 0.199	AB 3.642±0.404
MTX+Polymar 0.02	DE 3.9967±0.0985	C 4.638±0.2075	BC 2. 88±0.244
MTX+Polymar 0.05	DE 3.9785±0.176	C 4.631±0.198	BCD 2.04±0.199
MTX+Polymar 0.02+Lasser	CD 5.0012±0.1148	D 4.034±0.342	CD 2.983±0.193
MTX+Polymar 0.05+Lasser	CD 4.567±0.181	D 4.018±0.202	CD 3.007±0.501
MTX+Polymarpure±Lasser	B 5.3211±0.0693	D 3.6803±0.137	CD 3.021±0.328
LSD	0.199	0.401	0.602
-//P-value	«0.0005	«0.0005	«0.00005

Discussion of Sperm Result

According to the current study's I findings, the percentage I of sperm I motility I and the rate of sperm I concentration significantly decreased I in PANI-Fe_2O_3 mouse I treatment groups I. One of the research found that six months of exposure to PANI-Fe_2O_3 reduced the rate of sperm concentration I and motility. An imbalance I between the active I forms of oxygen I and antioxidants I results from oxidative stress caused by PANI-Fe_2O_3 in the sperm and semen. Additionally I, Fe_2O_3 reduces I the activity of antioxidant I enzymes I including Superoxide dismutase and Catalase, which results in the death of sperm and a reduction in sperm motility. [20] According I to a different research, giving I male rats a dosage of 0.05II

According I to the study, iron I oxide interacts with polyaniline I to produce active forms I of oxygen in male mice'sI testes. This increases I fat oxidation, which causes I a drop in sperm production and an I increase in sperm abnormalities in the treated I mice. II

According to the current study, the percentage of sperm motility significantly increased when PANIII-hybrid mice I were treated. II Glutathione I peroxidase has a crucial I role in the proper and efficient formation I of the midsection I of the sperm, as well I as in the mitochondria I and the nucleus of the sperm, and I it has been observed that I selenium increases I the effectiveness of antioxidant enzymes, including glutathione I peroxidase. III

5. Conclusion

Conductive iron nano powder can be used to make fertility-regulating compounds. The transport of sperm into the epididymis, a region that has been tested in vitro on mice and is useful for male contraception without having a lot of side effects, was thought to be affected by PANI and iron nano powder. The environment around the epididymis and spermatozoa are altered by the extract.

References

1. Hildebrandt, B.; Wust, P.; Ahlers, O.; Dieing, A.; Sreenivasa, G.; Kerner, T.; Felix, R.; Riess, H. The cellular and molecular basis of hyperthermia. Crit. Rev. Oncol. Hemat., 43, 33–56, (2002).
2. Schmidt, K.L.; Simon, E. Thermotherapy of pain, trauma, and inflammatory and degenerative rheumatic diseases. In Thermotherapy for Neoplasia, Inflammation, and Pain; Kosaka, M., Sugahara, T., Schmidt, K.L.,Simon, E., Eds.; Springer Japan: Tokyo, Japan, pp. 527–539, (2001).
3. Ibelli, T.; Templeton, S.; Levi-Polyachenko, N. Progress on utilizing hyperthermia for mitigating bacterial infections. Int. J. Hyperther., 34, 144–156. (2018)
4. Ashikbayeva, Z.; Tosi, D.; Balmassov, D.; Schena, E.; Saccomandi, P.; Inglezakis, V. Application of Nanoparticles and Nanomaterials in Thermal Ablation Therapy of Cancer. Nanomaterials (Basel) 2019,9, 1195.
5. V. Shanmugam, S. Selvakumar and C.-S. Yeh, Chem. Soc. Rev.,43,6254−6287, (2014).
6. S. Lal, S. E. Clare and N. J. Halas, Acc. Chem. Res., 2008, 41, 1842−1851.
7. L. Xu, L. Cheng, C. Wang, R. Peng and Z. Liu, Polym. Chem., 5, 1573−1580, (2014).
8. P. K. Jain, X. Huang, I. H. El-Sayed and M. A. El-Sayed, Acc. Chem. Res41, 1578−1586., (2008),
9. C. Wang, H. Tao, L. Cheng and Z. Liu, Biomaterials, (2011), 32, 6145−6154.
10. J. T. Robinson, S. M. Tabakman, Y. Liang, H. Wang, H. S. Casalongue,D. Vinh, and H. Dai, J. Am. Chem. Soc., , 133, 6825−6831(2011).
11. X. Huang, S. Tang, X. Mu, Y. Dai, G. Chen, Z. Zhou, F. Ruan, Z. Yang and N. Zheng, Nat. Nanotech., , 6, 28−32(2011).
12. Yijing Liu, Zhen Yang, Xiaolin Huang, Guocan Yu, Sheng Wang, Zijian Zhou, ZheyuShen, Wenpei Fan, Yi Liu, Matthew Davisson, Heather Kalish, Gang Niu, ZhihongNie, Xiaoyuan Chen. Glutathione-Responsive Self-Assembled Magnetic Gold Nanowreath for Enhanced Tumor Imaging and Imaging-Guided Photothermal Therapy. ACS Nano 12 (8), 8129-8137(2018), .
13. Barbero, H. Salavagione, D. Acevedo, D. Grumelli, F. Garay, G. Planes, G. Morales,M. Miras, Electrochim. Acta 49 3671–3686 (2004).
14. W. Dong, Y. Li, D. Niu , Z. Ma , J. Gu , Y. Chen , W. Zhao , X. Liu , C. Liu , J. Shi ,"Facile Synthesis of MonodisperseSuperparamagnetic Fe3O4 Core hybrid&Au Shell Nanocomposite for Bimodal Imaging and Photothermal Therapy" Adv. Mater., 23, 5392(2011).
15. L. Li, Y. Liu, P. Hao, Z. Wang, L. Fu, Z. Ma, J. Zhou, PEDOT nanocomposites mediated dual-modal photodynamic and photothermal targeted sterilization in both NIR I and II window, Biomaterials 41 132–140(2015).
16. Skotheim T, editor. Handbook of conducting polymers, I and II. New Marcel Dekker, (1986).
17. D. Jaque, L.M. Maestro, B. del Rosal, P. Haro-Gonzalez, A. Benayas, J.L. Plaza,E.M.

Rodríguez, J. GarcíaSolé, Nanoparticles for photothermaltherapies,Nanoscale 1–35(2014).
18. Amano K, Ishikawa H, Kobayashi A, Satoh M, Hasegawa E. Synth Met 1994;62:229.
19. L.E. Ibarra, E.I. Yslas, M.A. Molina, C.R. Rivarola, S. Romanini, C.A. Barbero,et al., Near-infrared mediated tumor destruction by photothermal effect of PANI-Np in vivo, Laser Phys. 23 066004–066007(2013).
20. J. Stejskal, A. Riede, D. Hlavata, J. Prokes, M. Helmstedt, P. Holler. Synth. Met. 96, 55 (2010).
21. Skotheim Watanabe,T WHO protocol MB-50. A Method for the Examining the Effect of a Plant Extract Administration Orally on the Fertility of Male Rats. World HealthOrganization (1983).
22. Subramanian, S., Rajendiran, G., Sekhar, P., Gowri, C., Govindarajulu, P. and Aruldhas, M.M. 1006.Reproductive toxicity of chromium in adult bonnet Monkeys (Macaca radiata Geoffrey). Reversible oxidative Stress in the semen. Toxicol.Appl. Pharmacol.,15; 215 (3) : 237 – 249 .
23. Ernst,E. and Bonde, JP. Sex hormones and epididymal sperm parameters in rats following sub –chronic treatment with hexavalent chromium.Hum.Exp. Toxicol., 11(4): 255 – 258(2010).
24. Kaur, P. and Bansal, M.P Influence of selenium induced oxidative stress on spermatogenesis and lactate dehydrogenase – X in mice testis (2004)
25. Watanabe,T. and Endo, . Effect of selenium deficiency on sperm morphology and spermatocyte chromosomes in mice. Mutat. Res., 262(2013): 93 – 99.